

PPV/TiO₂ hybrid composites prepared from PPV precursor reaction in aqueous media and their application in solar cells

Mingqing Wang, Xiaogong Wang*

Department of Chemical Engineering, Laboratory for Advanced Materials, Tsinghua University, Beijing 100084, PR China

Received 10 September 2007; received in revised form 23 January 2008; accepted 25 January 2008

Available online 1 February 2008

Abstract

In this work, poly(phenylene vinylene) (PPV) and TiO₂ nanocomposites containing different amounts of TiO₂ were prepared through PPV precursor reaction in aqueous media. The TiO₂ components were introduced into the systems by two methods, i.e. through in situ sol–gel reaction or by mixing commercially available TiO₂ nanoparticles with the PPV precursor before reaction. The composite prepared by mixing commercially available TiO₂ nanoparticles shows perfect crystal character of the anatase TiO₂, but TiO₂ particles severely agglomerate in the PPV matrix. The composite prepared by introducing TiO₂ nanoparticles through the sol–gel reaction shows uniform nanoscale dispersion of anatase TiO₂ in PPV matrix. The UV–vis and FL spectroscopic analyses confirm the formation of the TiO₂/PPV composites and reveal the enhanced PL quenching effect as the TiO₂ content increases. The PPV/TiO₂ composites can show significant photovoltaic response. Better photovoltaic performance is observed for the solar cells prepared by using the in situ sol–gel reaction method.

© 2008 Elsevier Ltd. All rights reserved.

Keywords: PPV/TiO₂; Nanocomposite; Photovoltaics

1. Introduction

Recently, nanocomposites of conjugated polymers (CPs) and inorganic compounds have been intensively investigated for the applications in devices such as light emitting diodes, photodiodes, sensors, smart microelectronic, and photovoltaic cells [1–3]. The nanocomposites can show novel synergic effects as well as enhanced optical and electronic properties. Hybrid CPs–SN (semiconductor nanocrystal) solar cells can combine interesting properties from CPs and bulk inorganic materials. The nanocomposites can show processing benefits of polymer-based materials such as the solution-processibility and low-temperature chemical synthesis. These advantages make them good candidate materials for clean, renewable and low-cost energy resources. The nanocomposites for hybrid solar cells have employed different SNs such as TiO₂ [4–6], ZnO [7–11], and CdSe [12–15].

To obtain high efficiency, it is ideal to have a bicontinuous interpenetrating network of electron-accepting and electron-donating components within the devices. Generally, the active layers of the polymer-based devices are prepared by using their solutions or dispersions. Conjugated polymers such as P3HT, P3OT, MEH–PPV and MDMO–PPV can be well dissolved in organic solvents and have been widely applied as the electron-donating and hole-transferring components in the photovoltaic materials. On the other hand, due to the increasing concern on environmental and safety problems related to the organic solvents, processing conjugated polymers by using aqueous media is getting increased importance. Recently, a water-soluble polythiophene (sodium poly(2-(3-thienyl)ethoxy-4-butylsulfonate), PTEBS) has been investigated for organic photovoltaics [16–19]. It is well known that PPV precursor has good solubility in aqueous media and can be converted into PPV by heating at high temperature (the Wessling–Zimmerman route) [20]. Therefore, PPV precursor could be used for preparing electron-donating component in aqueous media. To enhance the performance of PPV-based

* Corresponding author.

E-mail address: wxc-dce@mail.tsinghua.edu.cn (X. Wang).

composites, studies have been carried out on composites made of the polymers and nano-oxides recently [21,22].

In this work, PPV/TiO₂ composites were prepared through PPV precursor reaction in aqueous media. TiO₂ was used as the electron-accepting material because of its non-toxicity and abundance availability [23]. The TiO₂ components were introduced into the composites through in situ sol–gel reaction or by direct mixing of TiO₂ nanoparticle dispersions with the PPV precursor solutions. The PPV/TiO₂ composites were tested for photovoltaic device applications by sandwiching the active layers between a thin PEDOT layer and an aluminum top electrode. The preparation, characterization and photovoltaic properties of the nanocomposite materials will be presented in following sections in detail.

2. Experimental

2.1. Synthesis of PPV precursor

The PPV precursor was prepared according to the literature [24]. The monomer *p*-xylene-bis(tetrahydrothiophenium chloride) was prepared by reaction of dichloro-*p*-xylene (0.25 M) with excess tetrahydrothiophene (0.75 M) at 50 °C in methanol for 12 h. The product was purified by concentrating the reaction solution and then precipitating the condensed solution in cold acetone (0 °C). The solid was collected by filtration and dried thoroughly in vacuum oven. The PPV precursor was prepared by addition of 30 mL of 0.1 M NaOH solution into 30 mL of *p*-xylene-bis(tetrahydrothiophenium chloride) aqueous solution (0.1 M). Both solutions were cooled to 0 °C in an ice bath before mixing. The reaction proceeded at 0 °C for 1 h and then was terminated by the addition of 0.1 M HCl aqueous solution to neutralize the reaction solution. After the solution was concentrated, the PPV precursor aqueous solution was dialyzed against deionized water for several days. The PPV precursor was then freeze-dried and dissolved in water (20 mg/mL) for the following experiments.

2.2. Preparation of TiO₂ and PPV precursor mixtures

Method 1: TiO₂ dispersion with the solid content of 50 mg/mL was prepared by ultrasonication of nanoparticles (Degussa P25, average particle size 20 nm) in deionized water for 8 h. PPV precursor (20 mg/mL) was mixed with the TiO₂ dispersion in different ratios. The weight percentages of TiO₂ in PPV are given in Table 1. After mixing, the mixtures were further sonicated for 4 h to disperse the TiO₂ powder and prevent the dispersed powder from aggregating.

Table 1

The current–voltage characteristics of the hybrid photovoltaic cells with different TiO₂ contents prepared by direct mixing

TiO ₂ (wt%)	Thickness (μm)	<i>I</i> _{sc} (μA/cm ²)	<i>V</i> _{oc} (V)	FF	η (%)
20	1.22	17.55	1.15	0.21	0.004
40	1.26	35.1	1.18	0.21	0.009
60	1.32	58	0.86	0.2	0.010

Table 2

The current–voltage characteristics of the hybrid photovoltaic cells with different TiO₂ contents prepared by in situ sol–gel reaction

TiO ₂ (wt%)	Thickness (μm)	<i>I</i> _{sc} (μA/cm ²)	<i>V</i> _{oc} (V)	FF	η (%)
20	1.14	36.9	0.56	0.23	0.0048
40	1.16	139.7	0.46	0.26	0.018
60	1.18	118.5	0.35	0.22	0.009

Method 2: Ti(OC₃H₇)₄ (20 mL) was slowly dropped into 120 mL aqueous nitric acid solution (0.1 M) with strong stirring. The mixture was vigorously stirred at 80 °C for 8 h until a translucent solution was obtained. The solution was filtrated through a G4 filter to remove a small amount of yellow oil-like liquid and insoluble conglomerate. The sol solution containing TiO₂ particles was concentrated to 100 mg/mL and mixed with the PPV precursor solution (20 mg/mL) in different volume ratios. The weight percentages of TiO₂ in PPV are given in Table 2.

2.3. Substrate preparation

ITO glass slides covered with 50 nm thick poly(3,4-ethylenedioxythiophene) (PEDOT) were used as the solar cell substrates. The PEDOT films were prepared by electrodeposition in a three-electrode system (CHI660A Electrochemical Workstation). The ITO substrates were used as the electrodeposition working electrode and a saturated calomel electrode (SCE) was used as a reference electrode. PEDOT was deposited by the anodic deposition carried out in 50 mL boron trifluoride ether complex solution containing 0.355 g EDOT at 25 °C. Deposition current density and deposition time were 0.1 mA/cm² and 60 s, respectively.

2.4. Fabrication of solar cells

The mixtures prepared as above were cast-coated onto the PEDOT-covered ITO glass slides. After drying in an oven at 80 °C for 2 h, the composite films were subsequently placed in a vacuum oven at 200 °C for 6 h. In the process, PPV precursor was converted to PPV. For the sol–gel approach, the TiO₂ nanoparticles were formed in situ at the same time. The thickness of PPV/TiO₂ layers were measured by atomic force microscopy (AFM) and the results are given in Tables 1 and 2. Aluminum counter electrodes were deposited on the film surfaces by vacuum evaporation. The active areas of the cells were controlled to be 0.09 cm² with the adhesive transparent tapes before the thermal evaporation of aluminum.

2.5. Characterization

Composite films prepared by spin-coating on quartz substrates were used for the XRD and spectroscopic characterizations. XRD was performed on a Bruker D8-Discover instrument. Films for TEM observation were prepared by spin-coating on a 400 mesh copper grid. The TEM images

of the composite films were obtained by using a JEOL-JEM-1200EX microscope with an accelerating voltage of 120 kV. SEM measurement was performed on a field emission microscope (JEOL JSM-6301F) with the accelerating voltage of 5 kV. UV–vis spectra of the spin-coated films were recorded on a Perkin–Elmer Lambda Bio-40 spectrophotometer. Photoluminescence measurements were performed by using a Hitachi F-4500 fluorescence spectrophotometer. Current–voltage (I – V) measurements were carried out in air at room temperature using a Keithley 236 high current source power meter under white light with intensity of 100 mW/cm².

3. Results and discussion

The structure and schematic energy level diagram for the photovoltaic device are illustrated in Fig. 1. In the design, the PPV component was used as the electron donor and also for hole-transport. The PPV/TiO₂ composites were prepared from the PPV precursor in aqueous media through the Wessling–Zimmerman approach. The TiO₂ components were introduced into the composites through two different methods. In one of the methods, the composite was prepared through a modified sol–gel technique. In typical sol–gel approaches, TiO₂/polymer composites were prepared by using organic solvents [25,26]. In the current study, TiO₂ precursor was first hydrolyzed in aqueous solution and then mixed with PPV precursor in aqueous media. The applied method allows the inorganic materials to be synthesized at low temperatures without degrading the organic functional groups or polymers. This in situ formation scheme is designed to better disperse the nanostructured components. For comparison, PPV/TiO₂ composite was also prepared by mixing TiO₂ nanoparticle dispersions with PPV precursor solutions and then the PPV precursor was converted to PPV.

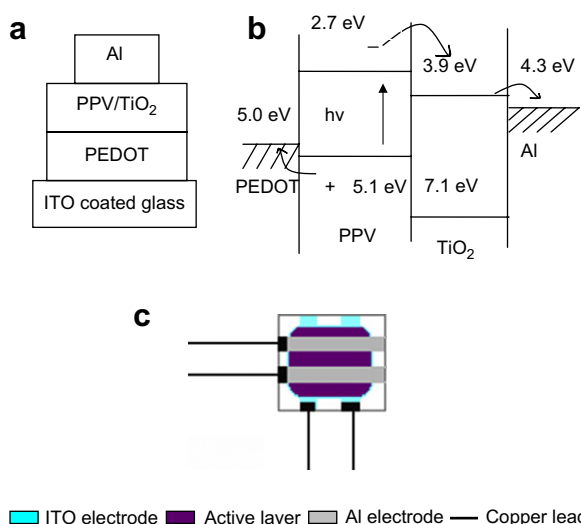


Fig. 1. (a) Layout of the PPV/TiO₂ photovoltaic devices, in which active layer is sandwiched between a PEDOT layer and aluminum top electrode. (b) Schematic energy level diagram for the device, where energy levels are given in eV relative to the vacuum level. (c) Schematic structure of one piece of solar cell device.

Fig. 2 shows the XRD patterns of the hybrid films with 60 wt% TiO₂ prepared by the two methods. In the figure, TiO₂ diffraction peaks can be assigned to the diffraction planes of the anatase phase according to the standard diffraction index. The peak at $2\theta = 25.3^\circ$ corresponds to the (101) crystal plane of anatase, others peaks at 38.1° , 48.1° , and 54.2° correspond to the anatase (112), (200), (211) crystal planes. As PPV component has a low crystallization degree, a broad diffraction peak related to the PPV component, which appears at $2\theta = 21.06^\circ$ [27], can be seen in the XRD figures (Fig. 2(a) and (b)). For the composite prepared by directly mixing TiO₂ nanoparticles with PPV precursor (Method 1), the crystallization of TiO₂ is perfect and the XRD curves is very similar to that of the pristine nanoparticles. The average crystallite size of TiO₂ phase was calculated to be 22 nm from the (211) reflection peak by the standard XRD software equipped on the instrument. For the composite prepared by the modified sol–gel method (Method 2), XRD curve also shows characteristic peaks of the anatase TiO₂, but the peaks are broader. In this preparation process, PPV precursor was blended with TiO₂ particle sol and the PPV/TiO₂ composite films were obtained by heating the mixture in a vacuum oven at 200 °C for 6 h. During the heating treatment, PPV precursor was converted to PPV and the crystallized TiO₂ was also formed at the same time.

In order to understand the XRD peak broadening of TiO₂ in the composites prepared by the sol–gel method, TiO₂ powder also was prepared by the sol–gel method under the similar conditions without the PPV-precursor/PPV matrix. Fig. 2(c) shows the XRD spectrum of the TiO₂ powder. Except the diffraction peak due to PPV, Fig. 2(b) and (c) shows very similar characteristic peaks of the anatase crystal. It can be seen that TiO₂ powder also shows the broad peaks similar to those given in Fig. 2(b). The result suggests that the PPV-precursor/PPV matrix shows little influence on the crystal structure of the TiO₂. The peak broadening is mainly due to the smaller crystallite domain and lower crystallization degree of TiO₂, which could be attributed to the low sol–gel reaction temperature used here. The average crystallite domain size of TiO₂ prepared by sol–gel method was calculated to be 12 nm from the (211) reflection peak by the standard XRD software.

The morphology and particle dispersion of the composites were investigated by TEM. Since the TiO₂ nanoparticles have the higher electron density, contrast between TiO₂-rich domains (darker) and PPV domains (lighter) can be clearly seen (Fig. 3). TEM images of the composites containing 40 wt% TiO₂ are given here as typical examples. Fig. 3(a) shows the PPV/TiO₂ composite prepared by direct mixing (Method 1). It can be seen that the TiO₂ nanoparticles aggregate severely to form clusters of ten to hundred nanometers. On the contrary, for PPV/TiO₂ composite prepared by in situ sol–gel reaction (Method 2), the TiO₂ particles are more uniformly dispersed in the PPV phase and show typical particle sizes in range from 10 to 20 nm. The size is in good agreement with the crystallite domain size estimated from XRD. It indicates that the TiO₂ nanoparticles are better dispersed in the PPV matrix by the sol–gel method. Fig 4 shows SEM images of PPV/TiO₂ composites with different contents (20, 40, and

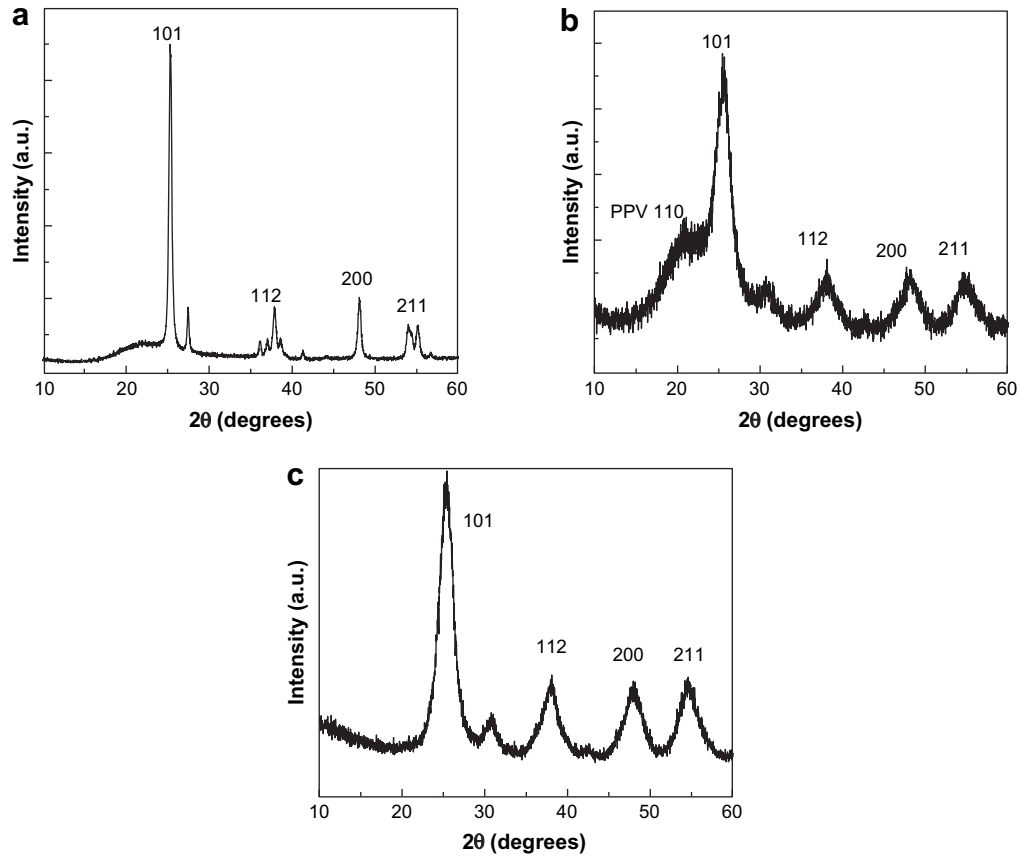


Fig. 2. X-ray diffraction of PPV/TiO₂ composites with 60 wt% TiO₂ prepared by (a) direct mixing, (b) in situ sol–gel reaction and (c) X-ray diffraction of TiO₂ nanoparticles prepared by sol–gel reaction.

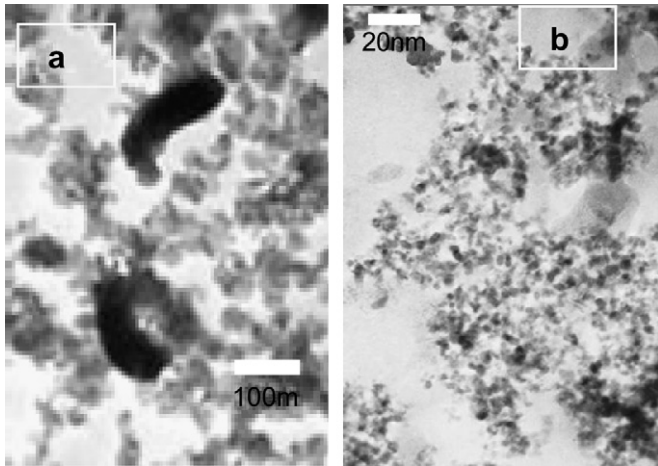


Fig. 3. TEM photographs of PPV/TiO₂ hybrid composites with 40 wt% TiO₂ prepared by (a) direct mixing and (b) in situ sol–gel reaction.

60 wt%) of TiO₂ nanoparticles prepared by direct mixing (Method 1). It can be seen that the TiO₂ phase in the hybrid materials are composed of the aggregates in significant amount.

Different dispersion states of TiO₂ nanoparticles in both kinds of the composites are related with the structures at the polymer/inorganics interface and the formation process of the TiO₂ nanoparticles. For the commercially available TiO₂ nanoparticles, some active bonds of TiO₂ on surfaces might

react with each other during the last annealing phase of the TiO₂ nanoparticle preparation. In the aqueous dispersions, the nanoparticles will agglomerate to decrease the surface area of the dispersed phase. This process is also favorable in energy as the van der Waals interaction between the nanocrystals is stronger compared to the weak interaction between TiO₂ nanoparticle and PPV precursor. When TiO₂ nanoparticles are formed in the in situ sol–gel process, TiO₂ precursor was partially hydrolyzed in aqueous solution, which will have strong interaction with PPV precursor in the media. This in situ formation nature can efficiently prevent TiO₂ nanoparticles from agglomeration.

UV–vis spectroscopy was used to investigate the effect of the TiO₂ amount and preparing method on the light absorption of composite films. Fig. 5 shows the UV–vis absorption spectra of PPV, PPV precursor, and spin-coated films of a series of PPV/TiO₂ nanocomposites. The PPV component shows absorption band with λ_{\max} around 400 nm (Fig. 5(a)) and TiO₂ absorbs light mainly in the wavelength range from 200 to 300 nm. As it can be seen from Fig. 5(b), the PPV/TiO₂ composites prepared by both methods show the overlapping absorption bands of PPV and TiO₂. The absorption intensity of TiO₂ increases with the increase of the TiO₂ content. By comparing the spectra, some differences can be seen from the UV–vis spectra of the composites obtained through different methods. For PPV/TiO₂ composites obtained by Method 1, the absorption band around 400 nm shows no difference as the

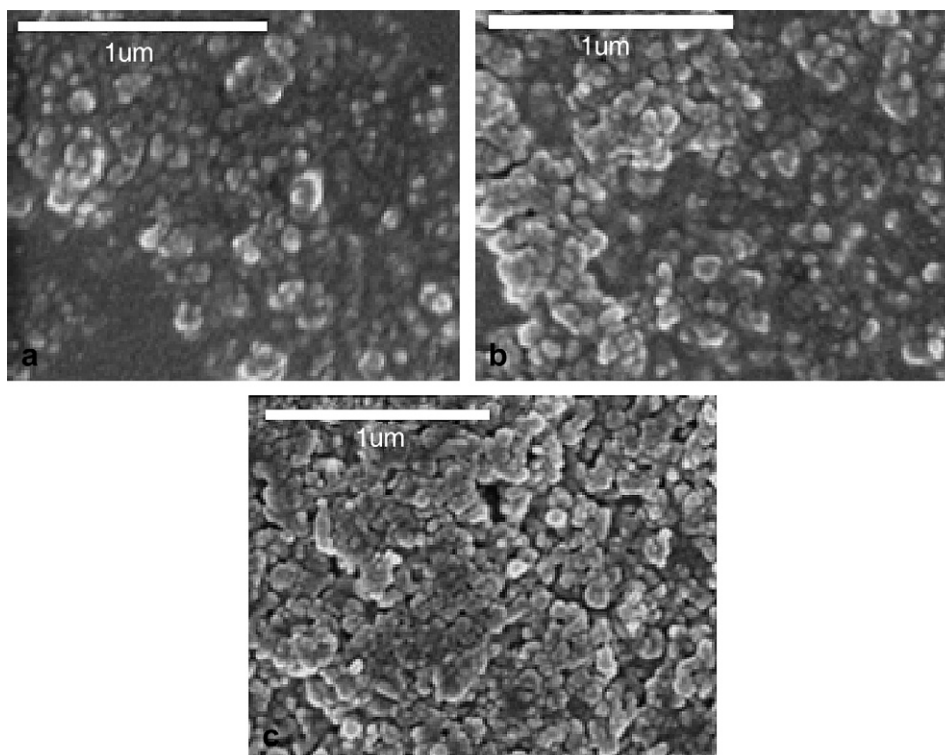


Fig. 4. SEM images of PPV/TiO₂ composites with different contents of TiO₂ nanoparticles prepared by direct mixing: (a) 20 wt%, (b) 40 wt%, (c) 60 wt%.

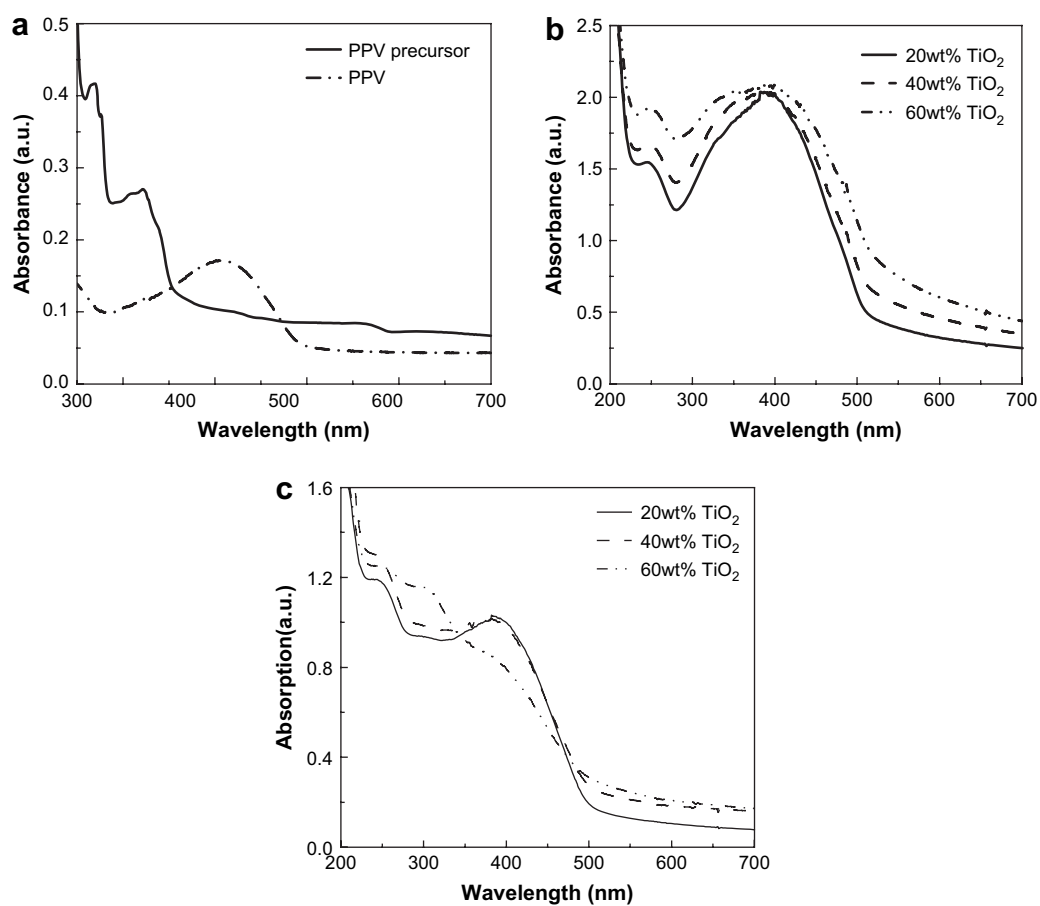


Fig. 5. UV-vis absorption spectra of PPV and PPV precursor (a), and PPV/TiO₂ nanocomposites with different TiO₂ contents prepared by direct mixing (b) and in situ sol-gel reaction (c).

TiO₂ content increases. For PPV/TiO₂ composites prepared by sol–gel method (Method 2), UV–vis absorption bands of PPV are very similar when TiO₂ contents are 20 wt% and 40 wt% but it significantly alters when TiO₂ content is increased to 60 wt% (Fig. 5(c)). The spectrum variation can be understood by comparing with the UV–vis spectrum of PPV precursor (Fig. 5(a)). It indicates that the spectral variation is most likely to be caused by the incomplete conversion from PPV precursor to PPV when the amount of the inorganic component is high.

Photoluminescence (PL) quenching can provide evidence of photo-induced charge transfer in PPV/TiO₂ composites. Fig. 6 shows PL spectra of PPV/TiO₂ composites with different amounts of TiO₂ prepared by the two methods. For the PPV/TiO₂ nanocomposites prepared by Method 1, the position of the emission peaks shows little change with the increase of the TiO₂ concentration but its intensity decreased significantly (Fig. 6(a)). For PPV/TiO₂ composites prepared by sol–gel method (Method 2), PL intensity of the composite films decreases more significantly as the TiO₂ content increases

(Fig. 6(b)). The enhanced PL quenching effect is mainly related to the composite morphology. In this case, the increased donor/acceptor interfacial areas and possible phase interpenetration can result in much more efficient PL quenching. On the other hand, this PL decrease could partially be due to the incomplete conversion of PPV precursor to PPV when the TiO₂ concentration is high.

The current density–voltage (*I*–*V*) characteristics of the PPV/TiO₂ composites devices are shown in Fig. 7. The short circuit current (*I*_{sc}) and open circuit voltage (*V*_{oc}) can be calculated from the intersection of the *I*–*V* curve on the ordinate and the crossing point of the curve with the abscissa. The fill factor, representing a measure of the quality of the *I*–*V* characteristic, can be calculated by

$$FF = (IV)_{\max}/V_{oc} \times I_{sc} \quad (1)$$

where $(IV)_{\max}$ is the maximum product of *I* and *V* that can be calculated from the *I*–*V* curve. The energy conversion efficiency, defined as the ratio of the electric power output of

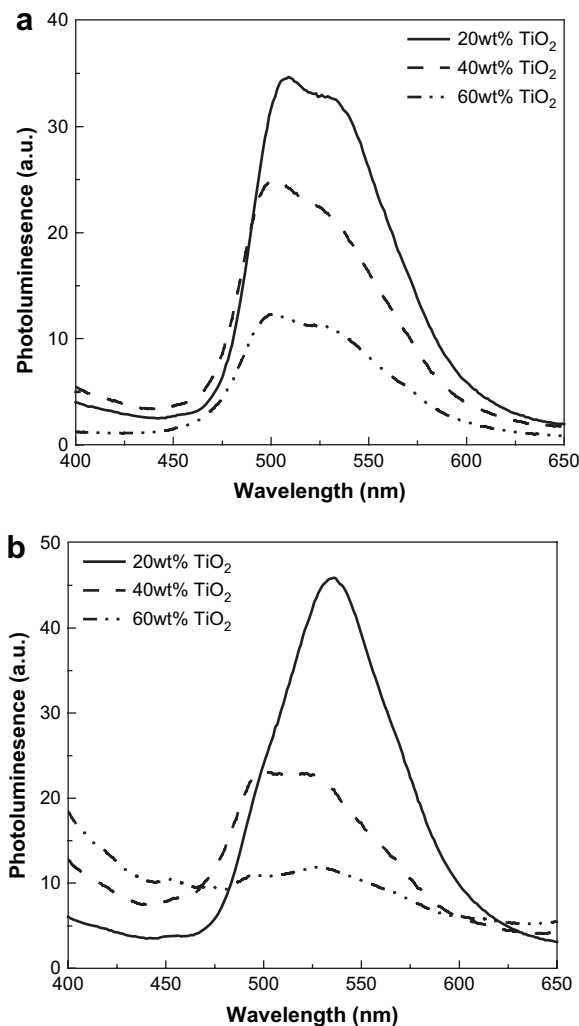


Fig. 6. Photoluminescence of PPV/TiO₂ nanocomposites with different TiO₂ contents prepared by direct mixing (a) and in situ sol–gel reaction (b).

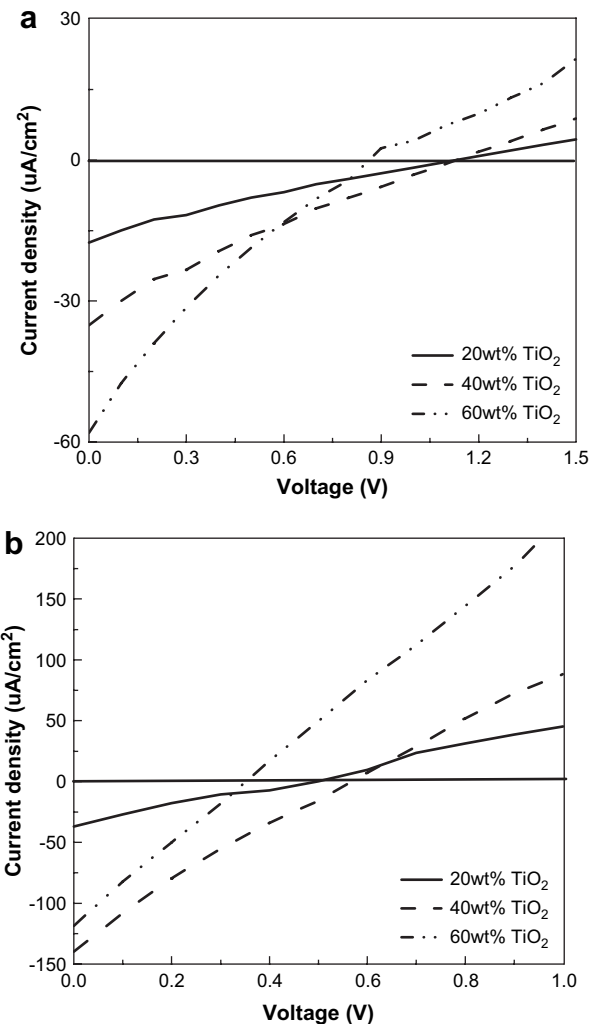


Fig. 7. Current density–voltage characterizations of photovoltaic devices based on PPV/TiO₂ nanocomposite with different TiO₂ contents prepared by direct mixing (a) and in situ sol–gel reaction (b).

the cell at the maximum power point to the incident optical power, can be obtained in terms of I_{sc} , V_{oc} , and FF by Eq. (2)

$$\eta(\lambda) = V_{oc} \times I_{sc} \times FF / P_{light} \quad (2)$$

Based on the equations given above, the parameters of the photovoltaic devices were derived from Fig. 7 and are summarized in Tables 1 and 2.

For the solar cells containing the active layers prepared by the two methods, both I_{sc} and V_{oc} of the devices are related to the TiO₂ contents in the composites. The high TiO₂ content can increase the electron donor/acceptor interfacial area to enhance exciton dissociation and form more percolation pathways for electron transfer at the same time. For the PPV/TiO₂ nanocomposites prepared by Method 1 (Fig. 7(a) and Table 1), I_{sc} and V_{oc} of the devices increase from 17.55 $\mu\text{A}/\text{cm}^2$ and 1.15 V to 35.1 $\mu\text{A}/\text{cm}^2$ and 1.18 V when TiO₂ content increases from 20 wt% to 40 wt%. But when the TiO₂ content further increases to 60 wt%, both V_{oc} and FF decrease slightly. This can be attributed to the increase of the aggregation when the TiO₂ content is high, as indicated by TEM observation. The aggregates in the photovoltaic active layer can trap the charge carriers and hinder the flow of the current, which leads to decrease of V_{oc} and FF. For PPV/TiO₂ composites prepared by sol–gel method (Fig. 7(b) and Table 2), the best performance can be observed for the composite with 40 wt% of TiO₂. This device shows V_{oc} of 0.46 V, I_{sc} of 139.7 $\mu\text{A}/\text{cm}^2$, FF of 0.26, and the efficiency of 0.018%. The higher efficiency compared to the composite prepared by direct mixing (Method 1) can be attributed to the nanosized phase separation, bicontinuous network, and possible interpenetrating phase structures. These factors can increase the interfacial areas between the PPV and TiO₂ and form more percolation pathways for the charge carriers, which results in the increase in the photoelectric conversion. However, when the TiO₂ content increases to 60 wt%, the photovoltaic cell performance becomes worse. The exact reason for the deterioration is still unclear. One possible reason is that the conversion from PPV precursor to PPV might not be completed when the amount of the inorganic component is high, which is implied by the UV–vis spectroscopic analysis. As a general result, the efficiency of the solar cells is low, which has also been reported for other photovoltaic cells prepared by using aqueous media [16–19].

Although the tested cells in this study show lower power conversion efficiencies in comparison with their counterparts prepared by using organic solvents, the results indicate that PPV/TiO₂ composite prepared in aqueous media can show significant photovoltaic response. Significant improvement on the photoelectric efficiency can be expected after the optimization at the compositions and the device structures. The preparation method can be potentially used in solar cell fabrication as a low-cost and environmentally friendly way.

4. Conclusion

In this work, PPV/TiO₂ hybrids were prepared through PPV precursor reaction in aqueous media. The TiO₂ nanoparticles

were introduced into the composites through direct mixing or a modified sol–gel method. The TiO₂ phase in the composites prepared by both methods possesses the characters of the anatase TiO₂. For the composite prepared by direct mixing, the severe aggregation of the TiO₂ nanoparticles can be observed. On the contrary, the composite prepared by the sol–gel method shows a nanosized phase separation. In comparison with those prepared by direct mixing, the devices containing the PPV/TiO₂ composites prepared by the sol–gel method show the significantly improved photovoltaic performance. The best performance can be observed for the device containing the composite with 40 wt% of TiO₂. The device shows V_{oc} of 0.46 V, I_{sc} of 139.7 $\mu\text{A}/\text{cm}^2$, FF of 0.26, and the efficiency of 0.018%.

References

- [1] Godovsky DY. *Adv Polym Sci* 2000;153:163–205.
- [2] Prasad PN. *Curr Opin Solid State Mater Sci* 2004;8(1):11–9.
- [3] Sudeep PK, Emrick T. *Polym Rev* 2007;47(2):155–63.
- [4] Arango AC, Johnson LR, Bliznyuk VN, Schlesinger Z, Carter SA, Horhold HH. *Adv Mater* 2000;12(22):1689–92.
- [5] Kwong CY, Choy WCH, Djuricic AB, Chui PC, Cheng KW, Chan WK. *Nanotechnology* 2004;15(7):1156–61.
- [6] Breeze AJ, Schlesinger Z, Carter SA, Brock PJ. *Phys Rev B* 2001;64(12):125205 [1–8].
- [7] Beek WJE, Wienk MM, Janssen RAJ. *Adv Mater* 2004;16(12):1009–13.
- [8] Coakley KM, Liu Y, Goh C, McGehee DM. *Mater Res Soc Bull* 2005;30:37.
- [9] Alem S, Bettignies RD, Nunzi JM. *Appl Phys Lett* 2004;84(12):2178–80.
- [10] Shaheen SE, Brabec CJ, Sariciftci NS, Padinger F, Fromherz JC, Hummelen T. *Appl Phys Lett* 2001;78(6):841–3.
- [11] Beek WJE, Wienk MM, Janssen RAJ. *J Mater Chem* 2005;15(29):2985–8.
- [12] Huynh WU, Dittmer JJ, Teclerian N, Milliro DJ, Alivisatos AP, Barnham KWJ. *Phys Rev B* 2003;67(11):115326 [12 pages].
- [13] Greenham NC, Peng X, Alivisatos AP. *Phys Rev B* 1996;54(24):17628–37.
- [14] Huynh WU, Dittmer JJ, Alivisatos AP. *Science* 2002;295(5564):2425–7.
- [15] Huynh WU, Dittmer JJ, Libby WC, Whiting GL, Alivisatos AP. *Adv Funct Mater* 2003;13(1):73–9.
- [16] McLeskey JT, Qiao QQ. *Int J Photoenergy* 2006;2006:1–6 [Article ID 20951].
- [17] Qiao QQ, Su LY, Beck J, McLeskey JT. *J Appl Phys* 2005;98:094906 [7 pages].
- [18] Qiao QQ, McLeskey JT. *Appl Phys Lett* 2005;86:153501–3.
- [19] Rud JA, Lovell LS, Senn JW, Qiao QQ, McLeskey JT. *J Mater Sci* 2005;40:1455–8.
- [20] Wessling RA, Zimmerman RG. *J Polym Sci Polym Symp* 1985;72:55–66.
- [21] Yang BD, Yoon KH, Chung KW. *Mater Chem Phys* 2004;83(2–3):334–9.
- [22] Yang SH, Nguyen TP, Rendu PL, Hsu CS. *Composites Part A* 2005;36(4):509–13.
- [23] Neugebauer H, Brabec C, Hummelen JC, Sariciftci NS. *Sol Energ Mater Sol Cell* 2000;61(1):35–42.
- [24] Gagnon DR, Capistran JD, Karasz FE, Lenz RW, Antonn S. *Polymer* 1987;28(4):567–71.
- [25] van Hal PA, Wienk MM, Kroon JM, Verhees WJH, Slooff LH, van Gennip WJH, et al. *Adv Mater* 2003;15(2):118–22.
- [26] Yang YN, Wang P. *Polymer* 2006;47(8):2683–8.
- [27] Chen D, Winokur MJ, Masse MA, Karasz FE. *Polymer* 1992;33(15):3116–22.